Density fluctuations and confinement in the Nagoya Bumpy Torus (NBT-1M)

A. Komori, H. Iguchi,[a] M. Fujiwara,[a] T. Shoji,[b] M. Hosokawa,[a] Y. Kawai, and H. Ikegami[a]
Interdisciplinary Graduate School of Engineering Sciences, Kyushu University, Kasuga, Fukuoka 816, Japan

(Received 27 September 1990; accepted 31 December 1990)

The stabilization of low-frequency density fluctuations is evidenced in the Nagoya Bumpy Torus (NBT-1M) [*Plasma Physics and Controlled Nuclear Fusion Research* (IAEA, Vienna, 1985), Vol. 2, p. 551] in the presence of microwave-heated hot-electron rings. Flute-type fluctuations, which are considered to be stabilized by the charge-uncovering effect of the rings, are found to cause large plasma losses, and to affect radial density profiles in the way that the lower fluctuation level yields the steeper density gradient. The particle confinement is, therefore, improved by the hot-electron rings to some extent, but is mainly determined by the plasma convection, which is expected from the discrepancy between density and potential profiles. It is also found that fluctuations in a toroidal plasma inside the ring grow when a weak negative ambipolar potential and a steep density gradient are formed, and are reduced to a low level when a deep potential well is achieved.

I. INTRODUCTION

The effect of hot-electron rings on the stability of plasmas has been the most important issue to be confirmed for the bumpy torus concept,[1] since the hot-electron rings[2] have been predicted to provide the average minimum-B configuration. Early experimental results indicated that the plasma was stable against low-frequency instabilities in the mode of operation designated the T mode, which was performed simultaneously with the formation of hot-electron rings.[3] In this mode, a negative potential well was observed, whose profile can be traced as a contour map of nested closed lines of equipotential.[4] However, recent experimental investigations have showed that the gradient B reversal is never achieved,[5] with the increased microwave power input of 90 kW into one mirror cavity, which is equivalent to the total input of 2.16 MW to the NBT-1M.[6] It has also been found that in the high-pressure mode of operation designated the C mode, the potential profile is characterized by the same contour plots as observed in a simple torus, resulting from charge separation due to toroidal drifts.[7,8] This indicates that the plasma confinement is not sufficiently improved even in the T mode,[9] compared with that in a simple torus, because the plasma confinement in the T and C modes does not differ extremely, in spite of the substantial difference between the potential profiles in these two modes.[8]

The larger experimental effort to prove the mechanism of the plasma confinement seems to result in the more confused observations. The purpose of the present study is to obtain a consistent picture about the plasma stability and confinement, clarifying the relationship between the hot electron rings and low-frequency fluctuations. High-frequency fluctuations have been also measured with magnetic probes, and the fluctuation of $\sim$23 MHz has been identified as a curvature-driven mode of hot-electron instabilities.[10] The hot-electron instabilities were considered to restrict low-pressure operation, and to destroy the plasma equilibrium, leading to the mode of operation designated M mode. Thus, the M mode has been observed at the lower pressure than the usual, accompanied by fluctuations, whose frequency is lower than 1 Hz, and whose fluctuation level is 100%. These features of the high-frequency fluctuations are almost the same as those reported in Ref. 11, and will be published elsewhere.

The experimental apparatus is described in Sec. II and the experimental results with possible interpretations are given in Sec. III. Conclusions are presented in Sec. IV.

II. EXPERIMENTAL ARRANGEMENT

Experiments have been performed on the NBT-1M (major radius of 140 cm), which is a toroidal confinement device consisting of 24 canted mirror cavities with an axial magnetic field **B** of 3.4–4.1 kG at the midplane.[12] The plasma is produced and heated by microwaves that are applied at the electron cyclotron harmonic frequencies. The duration of the discharge is 30 sec in our experiments. Hot-electron rings are created with second-harmonic electron cyclotron heating on the midplane of each mirror cavity. The microwave power P_μ is 30 kW at 18 GHz and 0–16 kW at 8.5 GHz. The lower frequency is used primarily to sustain the energetic ring electrons. For the present study, the NBT-1M is usually operated at B=4 kG and P_μ = 30 kW at 18 GHz. The microwave power P_μ at 8.5 GHz is fed in the experiments to obtain Figs. 7–9. Two distinct modes of operation are possible, depending on the values of P_μ and the neutral pressure p.[12] In our experi-

[a]Permanent address: National Institute for Fusion Science, Nagoya 464-01, Japan.
[b]Permanent address: Plasma Science Center, Nagoya University, Nagoya 464-01, Japan.

 0899-8221/91/041052-07$02.00

ments, the mode is controlled by changing p. At constant P_μ, the C and T modes are characteristic of high and low pressures, respectively.

Measurements of radial electron-density profiles and electron-density fluctuations were carried out at the midplanes of mirror cavities mainly with a neutral lithium-beam probe and a photodetector, respectively. The neutral lithium-beam probe was used to obtain the radial profiles of electron density n_e on the equatorial plane.[13] Electron-density fluctuations in the dc frequency range up to 300 kHz were measured with photomultiplier tubes (PMT's) having a frequency response above 500 kHz. The photomultiplier tube collects the H_α radiation that is dominant in the NBT-1M plasma, so that the output signal I_l is roughly proportional to $n_e lp$, where $n_e l$ is the electron line density, since, under our experimental conditions, the electron temperature T_e is higher than $\sim$40 eV and the neutral density is constant within 10%–20% across the plasma column. Thus, I_l carries information about line density fluctuations.[3] Two lines of sight were used; one was along the major axis of the torus (vertical view), and another was on the equatorial plane along a major radius (horizontal view). Radial profiles were obtained by changing the radial position of the vertical view.

III. EXPERIMENTAL RESULTS AND INTERPRETATION

A. Plasma convection

The radial profiles of electron density n_e are obtained with the neutral lithium-beam probe, as shown in Fig. 1(a), where the theoretically predicted locations of hot-electron rings are represented by the shadow areas. The plasma is found to consist of a toroidally confined plasma, surrounded by hot-electron rings, which in turn are surrounded by a surface plasma. With a decrease in p from 3.26×10^{-5} Torr to 2.11×10^{-5} Torr, n_e decreases and the n_e profile becomes flatter. However, at the C–T transition ($p\sim1.8\times10^{-5}$ Torr), n_e at $r\sim-1$ cm increases and a large gradient appears in the toroidal plasma. This change of the density profile at the C–T transition indicates that the particles are well confined, compared with those in the C mode, since the collisions become infrequent and nested closed contour plots of ambipolar potential begin to be formed. The plasma space potential ϕ_0 is controlled by the hot-electron rings, that is, by their loss mechanism.[6] Figure 1(b) shows the radial ϕ_0 profile in the T mode, measured with a heavy ion beam probe.[7] A potential well with a depth of $\sim$150 V is achieved, and the nested closed potential contours are formed around $r=-4$ cm. For the plasma confinement, the coincidence of the density and potential profiles is required, since such a large steady radial electric field E_0 will have a dominant effect on determining orbits of almost all particles in the NBT-1M under the present plasma parameters. In the early stage of the bumpy torus experiments, it had been considered that this condition is naturally satisfied and the deeper potential well yields the better plasma confinement. Thus, the large experimental effort was aimed at correlating the potential

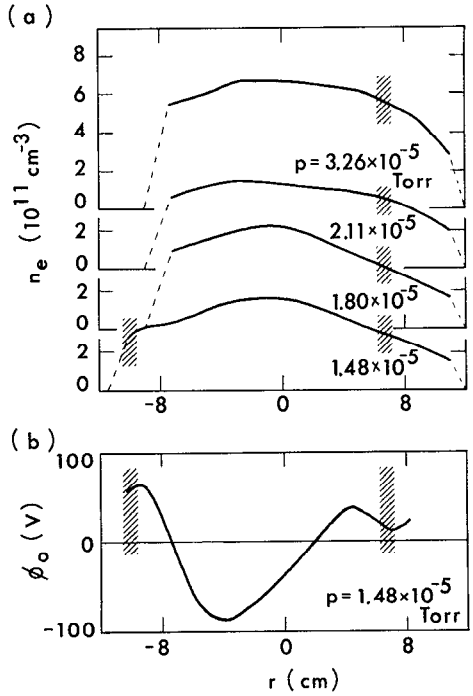

FIG. 1. Radial profiles of (a) electron density n_e at various neutral pressures, measured with a lithium-beam probe, and (b) space potential ϕ_0 obtained with a heavy ion beam probe. The shadow areas represent the theoretically predicted second-harmonic resonance regions for the primary heating power (18 GHz).

behavior and the hot-electron rings. However, it can be expected from Fig. 1 that the lines of equidensity and equipotential are displaced from each other; the center of the density contours is located around $r=-1$ cm, while that of the potential contours is located around $r=-4$ cm. This discrepancy then means that there is the plasma convection which leads to large plasma losses, and determines the global particle confinement. The potential well serves surely to cancel the charge separation due to the toroidal drifts, but on the other hand it enhances the plasma losses. Therefore, the extreme improvement of the plasma confinement is not realized by the formation of this potential well.

B. Plasma fluctuations

At first, a rough characterization of the plasma behavior is investigated by the line-integrated signals such as I_l and $n_e l$. The line density $n_e l$ is measured with a microwave interferometer. Figure 2 shows typical p dependence of $n_e l$ and the normalized fluctuation level $\tilde{I}_l/I_{0l}$ (the ratio of the root-mean-square amplitude $\tilde{I}_l$ to the time-averaged value I_{0l}), obtained with a horizontally viewing PMT. The level $\tilde{I}_l/I_{0l}$ is found to be almost constant as p decreases from 3.2×10^{-5} Torr to $\sim1.3\times10^{-5}$ Torr except for a small bump around $p=1.8\times10^{-5}$ Torr, which is always observed at the C–T transition. The level $\tilde{I}_l/I_{0l}$ has a tendency to grow at low pressure near the M mode. The bump of $\tilde{I}_l/I_{0l}$ is correlated well with the appearance of a

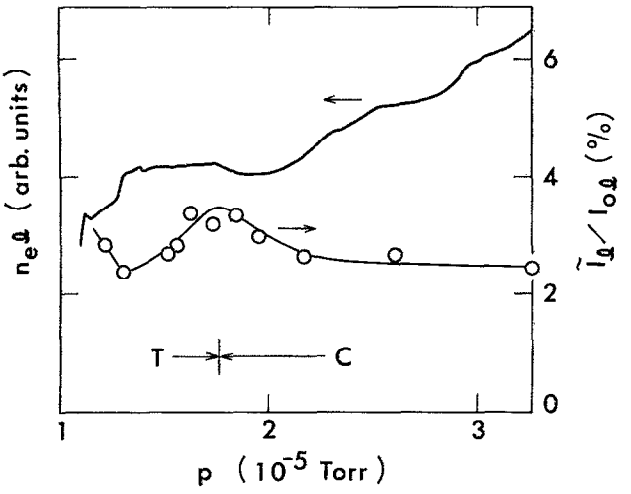

FIG. 2. Neutral pressure dependence of $n_e l$, measured with a microwave interferometer, and normalized fluctuation level $\tilde{I}_l/I_{0l}$ obtained with a horizontally viewing photomultiplier tube (PMT). These signals are integrated along the horizontal centerline. Modes of operation are indicated by T and C.

large density gradient and a weak negative ambipolar potential in the toroidal plasma at the C–T transition. When displayed on a spectrum analyzer, the $\tilde{I}_l$ fluctuations consist of low-frequency broadband oscillations and coherent modes, as shown in Fig. 3. The low-frequency broadband fluctuation has a maximum amplitude at the origin and decreases monotonically with increasing frequency. The coherent fluctuation is observed throughout the pressure

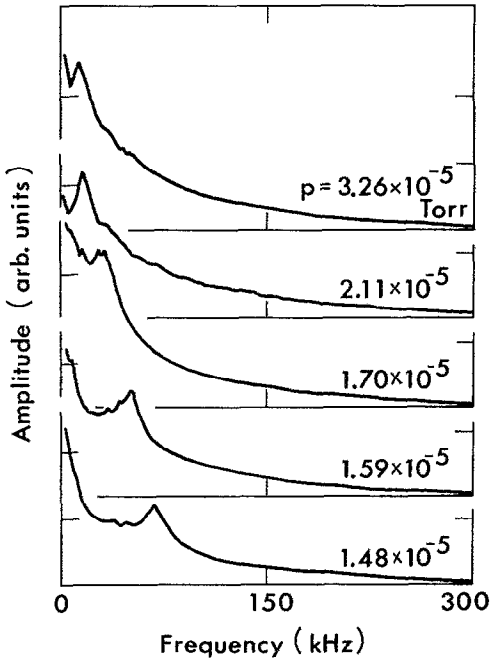

FIG. 3. Neutral pressure dependence of the frequency spectra of $\tilde{I}_l$. The spectrum amplitude scale is linear.

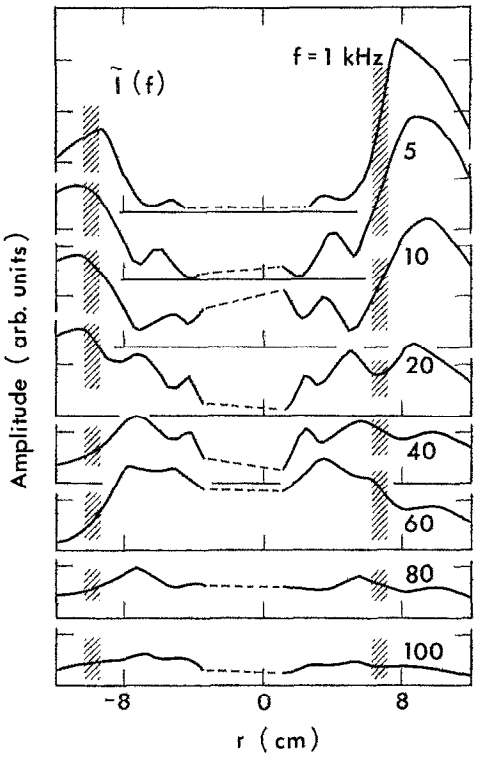

FIG. 4. Radial profiles of $\tilde{I}$ of 1, 5, 10, 20, 40, 60, 80, and 100 kHz fluctuations at $p=1.48\times10^{-5}$ Torr. This choice of the frequency does not mean that coherent fluctuations of 1, 5, ..., and 100 kHz are excited, except for the coherent fluctuation of 60 kHz.

regime, and the frequency increases as p is reduced in the T mode ($p\leqslant1.7\times10^{-5}$ Torr).

The radial profiles of local fluctuation level $\tilde{I}/I_0$ can be obtained from the Abel-inverted $\tilde{I}$ and I_0 signals, which are calculated from the radial profiles of $\tilde{I}_l$ and I_{0l}, measured with the vertically viewing PMT. The center of the conversion is taken at $r=0$ cm in the C mode, while at $r=-1$ cm in the T mode. It is found that the spatial distribution of $\tilde{I}/I_0$ is varied depending on p, although $\tilde{I}_l/I_{0l}$ is almost constant throughout the pressure regime, except at the C–T transition and near the M mode. Figure 4 shows the radial profiles of 1, 5, ..., and 100 kHz fluctuation amplitudes of $\tilde{I}$, obtained in the T mode. For example, the notation of $\tilde{I}$ (10 kHz) indicates that the signals are recovered after passing through a bandpass filter of 10 kHz center frequency, and not that a 10 kHz coherent fluctuation is excited. In this case, the bandwidth is chosen to be 300 Hz. The fluctuations of 1–10 kHz are found to be excited mainly in the surface plasma, but the fluctuation of 60 kHz is apparently observed in the steep density gradient region in the toroidal plasma, that is, inside the hot-electron rings. This frequency of 60 kHz agrees with that of the coherent fluctuation, observed in the frequency spectrum in the T mode ($p=1.48\times10^{-5}$ Torr). Thus, the low-frequency broadband fluctuations are excited mainly in the surface plasma, while the coherent fluctuations are observed in the toroidal plasma. The p dependence of the radial $\tilde{I}$ (5 kHz) profile indicates that the fluctuation am-

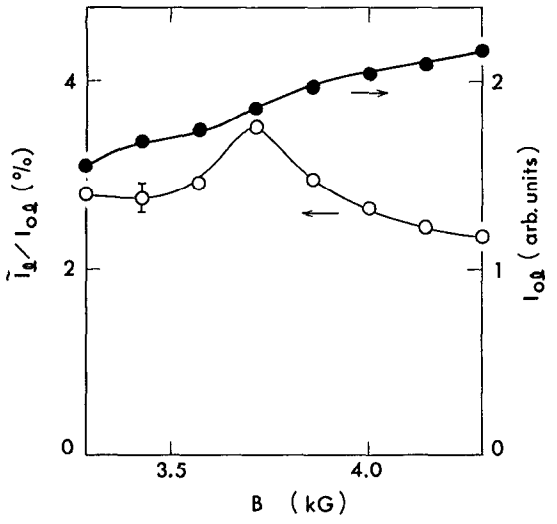

FIG. 5. Dependence of $\tilde{I}_l/I_{0l}$ and I_{0l}, measured with a horizontally viewing PMT, on the magnetic field B at $p=1.48\times10^{-5}$ Torr.

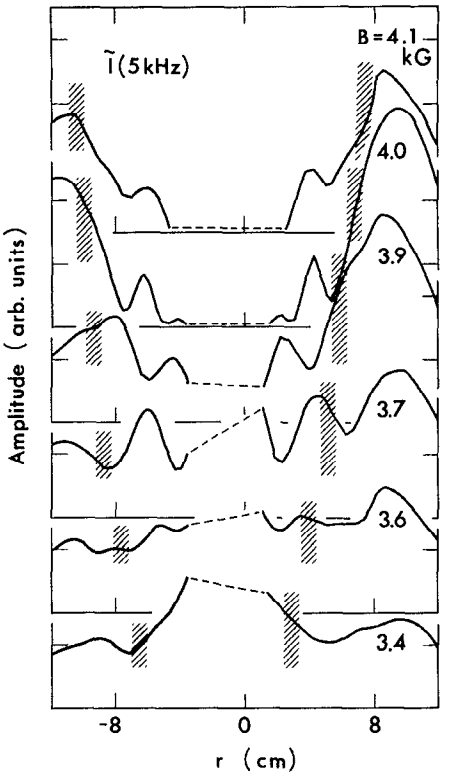

FIG. 6. Radial profiles of $\tilde{I}$ of 5 kHz fluctuations at various B's; $p=1.48\times10^{-5}$ Torr.

plitude in the toroidal plasma is as large as that in the surface plasma in the C mode. On the other hand, it is also shown that the radial amplitude profile of the coherent fluctuation is flat in the C mode. As p is reduced, these radial profiles change to the same characteristic profiles as observed in Fig. 4, respectively, depending on the frequency of the fluctuations. Therefore, it is clear that the frequency dependence of the radial profile of $\tilde{I}$, as shown in Fig. 4, is characteristic of the T mode, while the rather flat profile of $\tilde{I}$, which does not depend on the frequency of the fluctuations, is characteristic of the C mode.

Figure 5 shows the B dependence of $\tilde{I}_l/I_{0l}$, measured with the horizontally viewing PMT. With a decrease in B, $\tilde{I}_l/I_{0l}$ is observed to increase, and have a maximum at $B\sim3.7$ kG. A further decrease in B leads to the decrease in $\tilde{I}_l/I_{0l}$. The signal I_{0l} which is proportional to $n_e l$ decreases monotonically with a decrease in B, and it should be noted that I_{0l} decreases abruptly around $B=3.7$ kG, where $\tilde{I}_l/I_{0l}$ takes the maximum. The B dependence of the radial $\tilde{I}$ (5 kHz) profile is shown in Fig. 6. In the region of 3.9 kG$\leqslant B\leqslant$4.1 kG, the fluctuations are found to be excited mainly in the surface plasma, that is, outside the hot-electron rings, although the locations of hot-electron rings and fluctuations are shifted inward gradually with a decrease in B. However, the fluctuation appears apparently in the toroidal plasma at $B\sim3.7$ kG, and the radial $\tilde{I}$ (5 kHz) profile becomes rather flat as if in the C mode. This flat $\tilde{I}$ (5 kHz) profile is observed at the magnetic field below ~3.7 kG. The B dependence of the radial amplitude profile of the coherent fluctuation whose frequency is, roughly speaking, inversely proportional to B indicates that no large change of the profile occurs at $B\sim3.7$ kG. It is expected from these experimental results that the low-frequency broadband fluctuations are stabilized in the toroidal plasma when B is high, and that these fluctuations play an important role on the plasma transport, since large plasma losses are observed at the same time that the low-frequency broadband fluctuations appear in the toroidal plasma at $B\sim3.7$ kG. The coherent fluctuations are considered not to affect the plasma transport seriously, compared with the low-frequency broadband fluctuations. When B is lower than ~3.7 kG, the hot-electron rings lose the stabilization effect on the low-frequency broadband fluctuations, as mentioned above, and the plasma and fluctuations behave as if in the C mode. However, the difference of the plasma parameters between with and without hot-electron rings is not large in magnitude,[9] and large-amplitude MHD instabilities are not observed. The reason why the MHD instability is not excited under such a condition is considered to be that the plasma and wall are connected with a relatively short connection length, due to the plasma convection.

The role of the hot-electron rings on the fluctuations is examined by changing the microwave power at 8.5 GHz, P_μ (8.5 GHz). The fluctuation levels $\tilde{I}_l/I_{0l}$ measured with both the horizontally and vertically viewing PMT's are shown in Fig. 7, as a function of P_μ (8.5 GHz). At first, $\tilde{I}_l/I_{0l}$ decreases with an increase in P_μ (8.5 GHz) when P_μ(8.5 GHz) is low, and then increases abruptly at P_μ(8.5 GHz)$\sim$8 kW. The level $\tilde{I}_l/I_{0l}$ becomes low again, when P_μ (8.5 GHz) is higher than $\sim$12 kW. This dependence of $\tilde{I}_l/I_{0l}$ on P_μ (8.5 GHz) is correlated with the change of the n_e profile. Figure 8 shows the radial profiles of n_e and κ ($=-d\ln n_e/dr$) at P_μ (8.5 GHz) = 16 kW, together with those of $\tilde{I}$ (5 kHz) and $\tilde{I}$ (40 kHz). The additional shadows represent the theoretically predicted

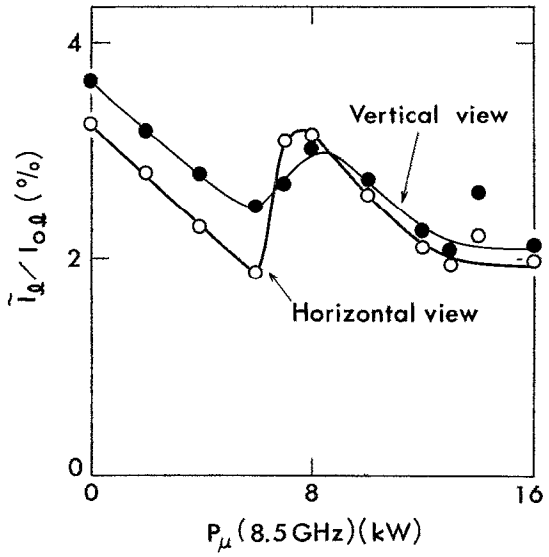

FIG. 7. Dependence of $\tilde{I}_{\parallel}/I_{0\parallel}$ measured with both horizontally and vertically viewing PMT's, on the microwave power at 8.5 GHz, P_μ (8.5 GHz); $B=3.9$ kG and $p=1.48\times10^{-5}$ Torr.

areas of electron cyclotron heating by the microwave at 8.5 GHz. In Fig. 8, the steeper density gradient than that shown in Fig. 1(a) is observed just inside the hot-electron rings. The abrupt increase in $\tilde{I}_{\parallel}/I_{0\parallel}$ at P_μ (8.5 GHz) ~ 8 kW occurs when the n_e profile is changed from the profile shown in Fig. 1(a) to that in Fig. 8. It is also found that the maximum density in the profile, which is located around $r=0$ cm, increases with an increase in P_μ (8.5 GHz), independently of the change of $\tilde{I}_{\parallel}/I_{0\parallel}$.

Figure 9 shows the dependence of the radial $\tilde{I}$ (5 kHz) profile on P_μ (8.5 GHz). A comparison of the radial profiles at P_μ (8.5 GHz) = 0 kW and at P_μ (8.5 GHz) = 16 kW indicates that when P_μ (8.5 GHz) is high enough, the low-frequency broadband fluctuations are stabilized in the toroidal plasma, and hence, there appear the steep density gradients, as shown in Fig. 8; this change in the radial $\tilde{I}$ (5 kHz) profile is apparently observed at $r=5$ cm and at $r=-8$ cm. From these experimental results, it is clear that the hot-electron ring can stabilize the low-frequency broadband fluctuations, and improve the particle confinement even if the average minimum-B configuration is not achieved by the rings. The low-frequency broadband fluctuation is considered to be stabilized by the "charge-uncovering" effect of the rings.[14] Another important result is that the inverse density gradient scale length κ, especially, in the region of 5 cm$\leqslant r\leqslant$8 cm, is correlated with the amplitude of the 5 kHz fluctuation in the manner that κ increases with a decrease in the fluctuation amplitude, as expected from Fig. 8. The similar relationship between κ and the squared density fluctuation level has been observed in the scrape-off layer of the TEXTOR tokamak, indicating that the radial particle diffusion in the scrape-off layer is caused mainly by fluctuations.[15] Thus, the observed relationship between κ and $\tilde{I}$ (5 kHz) suggests that the large cross-field flux is formed by the low-frequency broadband fluctuations, in addition to the plasma convection. The coherent fluctuation, observed in the toroidal plasma at P_μ (8.5 GHz) = 0 kW, is found to disappear at higher P_μ (8.5 GHz)'s than ~ 8 kW. However, the radial amplitude profiles of the fluctuations at frequencies above ~ 30 kHz are almost the same as those of the coherent fluctuations at

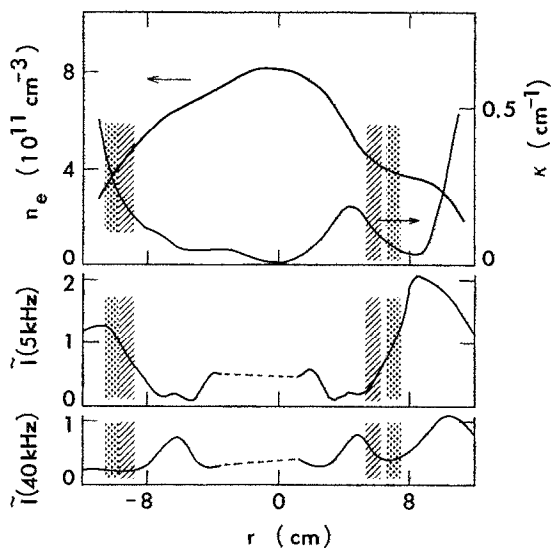

FIG. 8. Radial profiles of n_e, κ, $\tilde{I}$ (5 kHz), and $\tilde{I}$ (40 kHz); $B=3.9$ kG, P_μ (8.5 GHz) = 16 kW, and $p=1.48\times10^{-5}$ Torr.

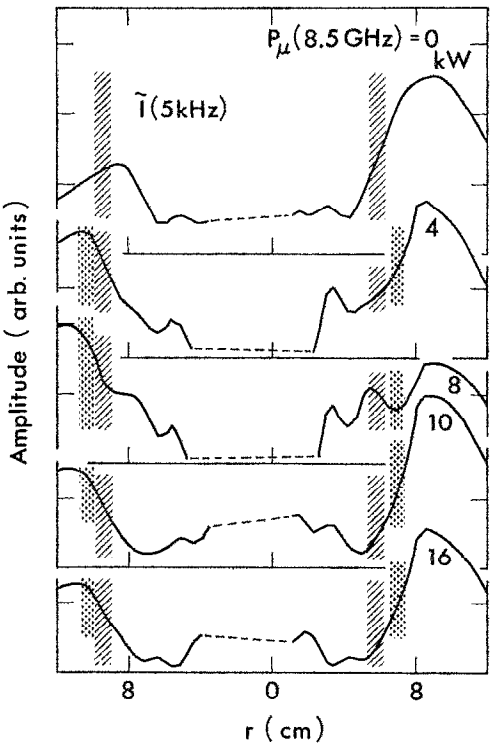

FIG. 9. Radial profiles of $\tilde{I}$ of 5 kHz fluctuation at various P_μ (8.5 GHz)'s; $B=3.9$ kG and $p=1.48\times10^{-5}$ Torr.

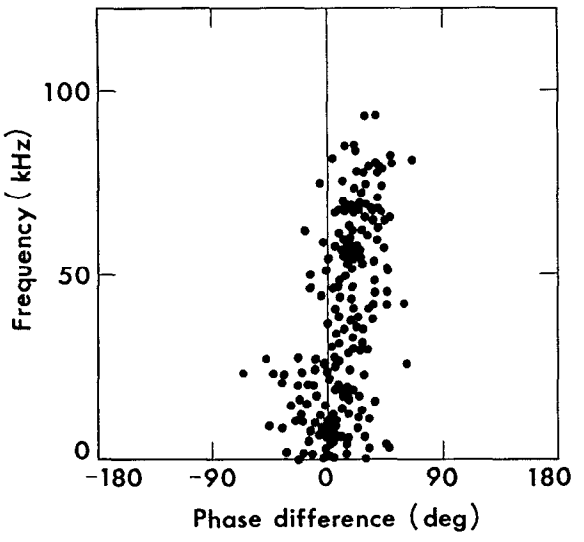

FIG. 10. Diagram of frequency versus phase difference between two $\tilde{I}_i$ signals, measured with two vertically viewing PMT's located 130° apart toroidally at $r=0$ cm; $p=1.48\times10^{-5}$ Torr, $B=3.9$ kG, and P_μ (8.5 GHz) = 0 kW.

P_μ (8.5 GHz) = 0 kW. These relatively high-frequency fluctuations whose amplitude is rather proportional to κ, as shown in Fig. 8, are considered to contribute to the increase in $\tilde{I}_i/I_{0i}$ at P_μ (8.5 GHz) ~ 8 kW, and not to affect the particle transport seriously, compared with the low-frequency broadband fluctuations, as mentioned before.

In order to know the wave features, the phase difference between the signals that were measured with the two vertically viewing PMT's located 130° apart toroidally at $r=0$ cm, was obtained by processing the signals with a fast Fourier transform. The sampling frequency was 1 MHz and the number of sampling points was 8192. A typical diagram of frequency versus phase difference in two perturbed $\tilde{I}_i$ signals in the T mode is shown in Fig. 10, where the fluctuations consist of many toroidal wave numbers, k_z's ($\propto$ the phase difference). The fluctuations at frequencies below ~10 kHz are substantially considered to have the wave features of flute modes because of $k_z \sim 0$°, while the fluctuations at frequencies above ~25 kHz, which seem to travel toroidally with an almost constant phase speed v_{ph}($= \omega/k_z$), have those of drift-wave-type instabilities since $k_z \neq 0$°. The points of the latter are concentrated at the frequency of ~60 kHz and at the phase difference of ~20°, corresponding to the coherent fluctuation in the toroidal plasma. Based on this phase difference, the toroidal and hence poloidal mode numbers of the coherent fluctuation are estimated to be $\frac{1}{6}$ and 6, respectively. The toroidal and poloidal wave numbers, k_z and k_y, are then obtained to be $\sim1.2\times10^{-3}$ cm^{-1} and ~1.2 cm^{-1}, respectively. The calculated frequency, ~53 kHz, of the coherent fluctuation agrees well with the observed frequency of ~60 kHz when the frequency shift caused by the $\mathbf{E}_0\times\mathbf{B}$ drift is included; the electron diamagnetic frequency is ~19 kHz at $T_e = 40$ eV, $B=4$ kG, $\kappa = 0.1$ cm^{-1} (at $r = 5$ cm), and $k_y = 1.2$ cm^{-1}, and the frequency shift due to the $\mathbf{E}_0\times\mathbf{B}$ drift is calculated to be ~34 kHz by estimating the effective E_0 to be about half of the electric field which is obtained from Fig. 1(b), since the coherent fluctuation is propagated across the potential well from one edge of the well to near the bottom of the well, as expected from Figs. 1(b) and 4. The observed k_z also agrees with the calculated k_z of $\sim4.5\times10^{-4}$ cm^{-1} at $\omega/2\pi = 19$ kHz within a factor of 3. This calculated k_z is given by $k_z \sim \omega/v_e$ (v_e is $\sqrt{T_e/m_e}$), and known to give the maximum growth rate of the collisionless drift wave.[16]

The coherent fluctuation in the toroidal plasma is found to grow at the C–T transition, as mentioned before, when a steep density gradient and a shallow potential well are formed. As p is decreased, the fluctuation is reduced to a low level. An important point is that E_0 becomes large with a decrease in p, while κ is little changed, so that E_0 is considered to play an important role on controlling the coherent fluctuations in the toroidal plasma. This E_0 dependence of the fluctuation amplitude agrees qualitatively with the theoretical prediction for the drift wave.[17]

IV. CONCLUSIONS

The basic conclusion of the present studies is that the hot-electron rings can stabilize the low-frequency fluctuations, in spite of the fact that the average minimum-B configuration is not achieved by the rings. This is not so surprising, because the charge-uncovering effect of the ring is considered to stabilize the flute modes which play an important role on the particle transport. It is found that the inverse density gradient scale length κ increases monotonically with a decrease in the fluctuation amplitude. This relationship between κ and the fluctuation amplitude is similar to that observed in the scrape-off layer of the TEXTOR tokamak, and means that there is a cross-field flux caused by the fluctuations. Drift-wave-type fluctuations which are excited mainly inside the hot-electron ring, can also be controlled by the ambipolar potential formed by the hot-electron rings in the way that the fluctuation amplitude grows at a weak negative ambipolar potential, and is reduced to a low level when a deep potential well is achieved. MHD instabilities are not observed in the T mode even if the hot-electron rings are not formed, because the plasma and wall are connected with a relatively short connection length, due to the plasma convection.

Since the hot-electron ring stabilizes the low-frequency fluctuations both in the toroidal and surface plasmas, as mentioned above, the hot-electron ring might improve the particle confinement amazingly if we could make a device where contour plots of density agree with those of potential.

ACKNOWLEDGMENTS

The authors wish to thank H. Sanuki, T. Kamimura, M. Tanaka, and F. Tsuboi for many illuminating discussions, K. Takasugi and A. Tsushima for help with the data analysis using a computer, and C. Takahashi and T. Takita for their technical support. One of us (A.K.) is grateful to N. Sato for his continuing encouragement.

[1] R. A. Dandl, H. O. Eason, A. C. England, G. E. Guest, C. L. Hedrick, H. Ikegami, and D. B. Nelson, in *Plasma Physics and Controlled Nuclear Fusion Research* (IAEA, Vienna, 1975), Vol. 2, p. 141; E. F. Jaeger, D. A. Spong, and C. L. Hedrick, Phys. Rev. Lett. **40**, 866 (1978).
[2] H. Ikegami, H. Ikezi, M. Hosokawa, S. Tanaka, and K. Takayama, Phys. Rev. Lett. **19**, 779 (1967); R. A. Dandl, H. O. Eason, P. H. Edmonds, and A. C. England, Nucl. Fusion **11**, 411 (1971); D. B. Nelson and C. L. Hedrick, *ibid.* **24**, 1173 (1984).
[3] A. Komori, Nucl. Fusion **24**, 1173 (1984).
[4] F. M. Bieniosek and K. A. Connor, Phys. Fluids **26**, 2256 (1983).
[5] K. Kadota, C. Takahashi, H. Iguchi, M. Fujiwara, K. Matsunaga, and J. Fujita, Rev. Sci. Instrum. **56**, 857 (1985).
[6] H. Ikegami, M. Hosokawa, H. Iguchi, T. Shoji, T. Kamimura, H. Sanuki, K. Takasugi, F. Tsuboi, T. Takeuchi, A. Komori, K. Kadota, J. Fujita, C. Honda, M. Yokoo, M. Maeda, K. Muraoka, T. Yuyama, T. Michishita, H. Kubo, and M. Fujiwara, in *Plasma Physics and Controlled Nuclear Fusion Research* (IAEA, Vienna, 1987), Vol. 2, p. 489.
[7] K. Takasugi, J. Phys. Soc. Jpn. **53**, 2546 (1984).
[8] S. Hiroe, J. C. Glowienka, D. L. Hillis, J. B. Wilgen, G. L. Chen, J. A. Cobble, A. M. El Nadi, J. R. Goyer, L. Solensten, W. H. Casson, O. E. Hankins, and B. H. Quon, Phys. Fluids **30**, 848 (1987).
[9] D. L. Hillis, J. B. Wilgen, J. A. Cobble, S. Hiroe, W. A. Davis, D. A. Rasmussen, R. K. Richards, T. Uckan, E. F. Jaeger, O. E. Hankins, J. R. Goyer, and L. Solensten, Phys. Fluids **28**, 2848 (1985).
[10] H. L. Berk, J. W. Van Dam, M. N. Rosenbluth, and D. A. Spong, Phys. Fluids **26**, 201 (1983).
[11] S. Hiroe, J. B. Wilgen, F. W. Baity, L. A. Berry, R. J. Colchin, W. A. Davis, A. M. El Nadi, G. R. Haste, D. L. Hillis, D. A. Spong, and T. Uckan, Phys. Fluids **27**, 1019 (1984).
[12] M. Fujiwara, T. Kamimura, M. Hosokawa, T. Shoji, H. Iguchi, H. Sanuki, K. Takasugi, F. Tsuboi, H. Tsuchidate, K. Kadota, K. Matsunaga, K. Sato, K. Tsuchida, A. Tsushima, and H. Ikegami, in *Plasma Physics and Controlled Nuclear Fusion Research* (IAEA, Vienna, 1985), Vol. 2, p. 551.
[13] H. Iguchi, K. Kadota, K. Takasugi, T. Shoji, M. Hosokawa, M. Fujiwara, and H. Ikegami, Rev. Sci. Instrum. **56**, 1050 (1985).
[14] H. Sanuki and F. F. Chen, Phys. Fluids **28**, 3567 (1985).
[15] A. Komori, O. Mitarai, K. Yamagiwa, C. Honda, K. Kadota, J. Fujita, Y. T. Lie, U. Samm, A. Pospieszczyk, K. Höthker, P. Bogen, and E. Hintz, Nucl. Fusion **28**, 1460 (1988); A. Komori, S. Masamune, O. Mitarai, K. Yamagiwa, C. Honda, K. Kadota, J. Fujita, Y. T. Lie, and U. Samm, J. Nucl. Mater. **162–164**, 231 (1989).
[16] A. Komori and N. Sato, Jpn. J. Appl. Phys. **23**, 475 (1984).
[17] H. Sanuki, Phys. Fluids **27**, 2500 (1984).